Available online at www.sciencedirect.com
SCIENCE DIRECT®
ELSEVIER
International Journal of Impact Engineering 31 (2005) 735–754
INTERNATIONAL JOURNAL OF IMPACT ENGINEERING
www.elsevier.com/locate/ijimpeng

Constitutive equation for Ti–6Al–4V at high temperatures measured using the SHPB technique

Songwon Seo[a,*], Oakkey Min[b], Hyunmo Yang[a]

[a] *Department of Mechanical Engineering, Graduate School, Yonsei University, 134 Shinchon-dong, Seodaemum-gu, Seoul 120749, Republic of Korea*

[b] *School of Mechanical Engineering, Yonsei University, 134 Shinchon-dong, Seodaemum-gu, Seoul 120749, Republic of Korea*

Received 25 February 2003; accepted 4 April 2004

Available online 14 August 2004

Abstract

A high temperature split Hopkinson pressure bar (SHPB) test system is used to investigate the effects of temperature as well as those of strain and strain-rate. Effects of temperature for the titanium alloy (Ti–6Al–4V) are investigated by developing a high temperature SHPB test system. In this work, high temperatures greater than 1000°C are attained in the SHPB test specimens by using two ellipsoidal radiant heating reflectors with two halogen lamps. The thermal gradients in the specimens are observed as they are heated. Methods for solving problems related to conduction between the specimens and elastic bars and techniques for measuring the temperature of the specimens are suggested. When testing with the high-temperature SHPB apparatus, care is required to prevent oxidation of the surface of the specimen, and to prevent an inhomogeneous temperature distribution from developing in the specimen. To determine the true flow stress–true strain relationship, specimens are tested from room temperature to 1000°C at intervals of 200°C and at a strain-rate of 1400 s^{-1}. The parameters for a Johnson–Cook constitutive equation and a modified Johnson–Cook constitutive equation are determined from the test results. The modified Johnson–Cook constitutive equation is more suitable for expressing the dynamic behavior of the Ti–6Al–4V titanium alloy in the vicinity of the recrystallization temperature.

Keywords: SHPB; Radiant heating; High temperature; High strain-rate; Johnson–Cook constitutive equation

*Corresponding author. Tel.: +82-2-2123-2817; fax: +82-2-362-2736.
E-mail address: spacexman@hotmail.com (S. Seo).

0734-743X/$ - see front matter © 2004 Elsevier Ltd. All rights reserved.
doi:10.1016/j.ijimpeng.2004.04.010

1. Introduction

Material properties generally differ between dynamic and static states. The dynamic mechanical properties of a material are known to be dependent on the strain, strain-rate, and temperature. The split Hopkinson pressure bar (SHPB) technique has been widely used to study the dynamic behavior of materials at high strain-rates [1–3]. The experimental concepts of the technique, which is commonly used for strain-rates ranging between 10^2 and 10^4 s^{-1}, were first introduced by Hopkinson [4] in 1914. The practical configuration, which consists of a short specimen between two long bars and is widely used today, was devised by Kolsky [5] and developed by Davies and Hunter [6] and Lindholm [1], as well as others. The strain-rate and temperature sensitivities of the specimen interact because the flow stress in a metal increases as the strain-rate increases, and decreases as the temperature increases. The SHPB technique has been used to characterize material properties at high strain-rates and high temperatures [2,7–13], and several types of high-temperature SHPB system have been developed to investigate the behavior of materials at high temperature ranges.

Chiddister and Malvern [7] performed pioneering experiments between room and high temperatures ($30 \sim 550^{\circ}C$) using a SHPB apparatus. An electric combustion tube furnace was used to heat the specimens, and a thermocouple was welded to the transmitter bar to monitor the specimen temperature. Because a portion of the pressure bars was heated with the specimen due to the structure of the furnace, they used a method whereby the temperature distribution was measured with additional thermocouples at uniform intervals, and then the amplitude of the stress measurements was corrected to take into account transmission through the thermal gradient. However, such techniques have limitations on the attainable specimen temperature; these are imposed by heat conduction in the bars and by the properties of the bar material at very high temperatures. The thermal cycling associated with repeated testing can also permanently alter the mechanical properties of the bars [11].

Follansbee et al. [2] used a furnace to heat the specimen. Each specimen was heated in the furnace for a few minutes to achieve thermal equilibrium and ensure a uniform temperature distribution. However, the pressure bars in their SHPB apparatus were designed to be installed near the furnace, so undesirable heat conduction may have occurred. Thermal gradients in the pressure bars may cause changes in the mechanical impedance, such as the longitudinal wave speed and Young's modulus. A change in the mechanical impedance will yield the reflection and dispersions of the wave. Macdougall [12,13] first used a radiant heater to heat the specimen. A radiant heater is capable of concentrating heat energy on the specimen so that the heating time is shorter than that obtained using a furnace.

In this paper, a radiant heating system was developed to heat the specimen. Methods for solving problems that were encountered between the specimen and elastic bars, and techniques for measuring the temperature of the specimen will be discussed. The pressure bars used in this study were made from Inconnel 718 to reduce the change of the mechanical impedance at the end faces when the bars were in contact with the high temperature specimen. Inconel 718 has low-temperature dependence of Young's modulus. To investigate the effects of temperature as well as strain and strain-rate, the titanium alloy Ti–6A1–4V was selected as the high-temperature SHPB test material. This alloy is commonly used for airframes, turbine blades, etc. A constitutive equation of the test material expresses the true flow stress and true strain data measured by the

high-temperature SHPB apparatus. The Johnson–Cook equation and the modified Johnson–Cook equation, which have been most widely used for material constitutive equations, were chosen to represent the behavior of the test material.

2. Experimental techniques

2.1. Theory

The theory of the SHPB procedure is based on one-dimensional wave propagation in aligned bars, as shown in Fig. 1. When a striker bar impacts an incident bar, a compressive elastic wave travels through the incident bar. When this wave reaches the specimen, some portion of the wave is reflected at the specimen surface, while the remaining portion travels through the transmitter bar. The traveling waves can be measured by strain gages and a signal conditioner. Three equations are required to calculate the true flow stress–true strain relationship of a test material from the experimental strain data [1],

$$\dot{\varepsilon}(t) = -\frac{2C}{L}\varepsilon_{\mathrm{R}}(t), \tag{1}$$

$$\varepsilon(t) = -\frac{2C}{L}\int_0^t \varepsilon_{\mathrm{R}}(t')\,\mathrm{d}t', \tag{2}$$

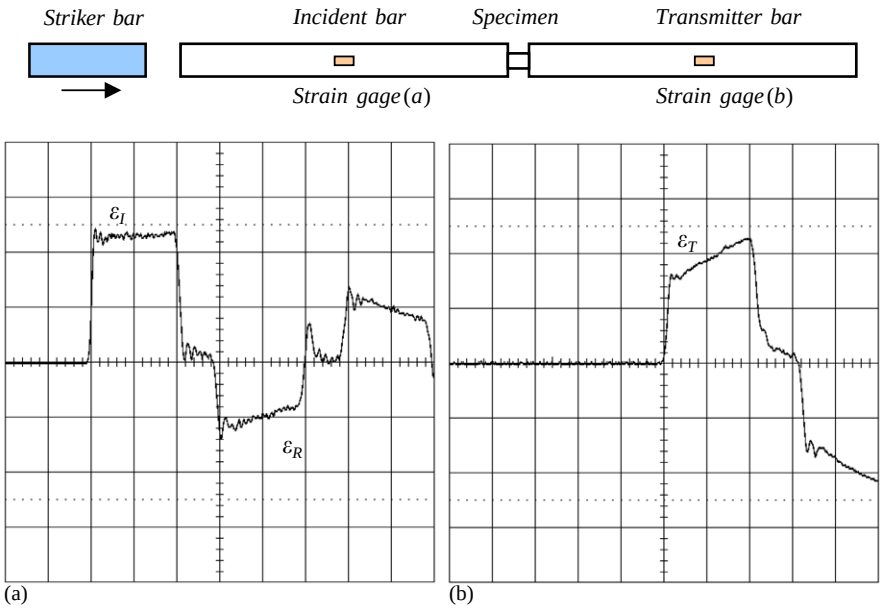

Fig. 1. One-dimensional alignments of the elastic bar and specimen and strain histories in the (a) incident bar and (b) transmitter bar.

$$\sigma = E\frac{A_b}{A}\varepsilon_T(t), \tag{3}$$

where $\dot{\varepsilon}(t)$ denotes the strain-rate, $\varepsilon(t)$ is the strain, σ is the flow stress, C is the speed of the elastic wave in the elastic bars, L is the length of the specimen changed by deformation, A_b is the cross sectional area of the elastic bars, A is the cross sectional area of the specimen, E is Young's modulus of the elastic bars, and ε_I, ε_R, and ε_T are the incident, reflected, and transmitted waves, respectively. The strain in the incident bar ε_I can be expressed in terms of ε_R and ε_T, and therefore does not appear in Eqs. (1)–(3). The strain histories of the incident wave (ε_I) and reflected wave (ε_R) from the incident bar, and the strain histories of the transmitted wave (ε_T) from the transmitter bar, are shown in Fig. 1.

As a specimen with an initial length L_0 and an initial cross sectional area A_0 at $t = 0$ deforms, its length L decreases and its cross sectional area A increases as $t > 0$. The current length and cross sectional area of the specimen with time can be obtained by using the constant volume condition for plastic deformation, expressed as

$$V_0 = A_0L_0 = AL, \tag{4}$$

where V_0 is the initial volume of the specimen. From the relationship between the true strain, calculated from Eq. (2), and the length of the specimen, i.e., $\varepsilon(t) = \ln(L/L_0)$, the length of the specimen at time t can be computed using

$$L = L_0e^{\varepsilon(t)}. \tag{5}$$

We can also obtain the cross sectional area of the specimen at time t from the relationship given by Eq. (4),

$$A = \frac{L_0}{L}A_0. \tag{6}$$

Therefore, the flow stress–strain relationship of a material can be determined using the experimental values of ε_R and ε_T, and Eqs. (1)–(3).

2.2. SHPB experimental system

The compressive SHPB system for high temperature tests consists of two pressure bars, an impact loading apparatus, a heater system, and measuring instruments [14]. A schematic diagram of the test system used in this work is shown in Fig. 2. The incident bar, transmitter bar, and striker bar were made of Inconel 718, and were 20.6375 mm (13/16 in) in diameter. Each pressure bar was 1500 mm in length, and the striker bar was 500 mm in length. A launching device was used to accelerate the striker bar to produce a compressive impact wave on the incident bar. Compressed nitrogen gas was employed to accelerate the striker bar. Several measurement devices were adopted to measure the strain voltages, velocity of the striker bar, and temperature of the specimen.

2.2.1. Heater

A non-contact heating system was required to heat the specimen in order to measure the flow stress-strain relationship at high temperatures. The adopted radiant heating system consisted of

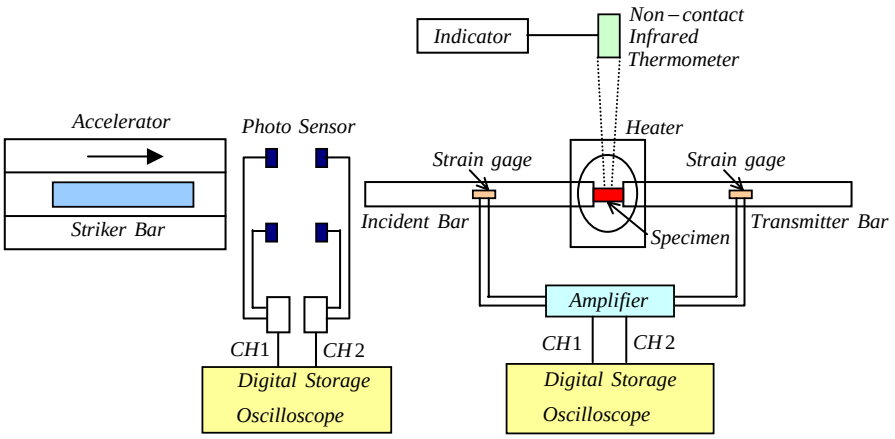

Fig. 2. Schematic diagram of the high-temperature compressive SHPB apparatus.

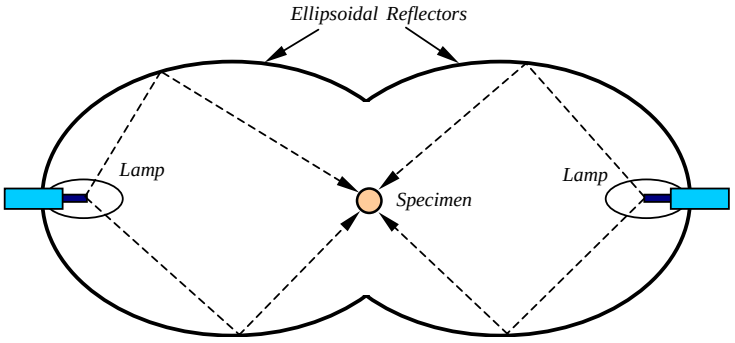

Fig. 3. Schematic diagram of the radiant heating system.

two ellipsoidal aluminum reflectors and two tungsten filament halogen lamps (650 W). The concept of the radiant heating system used in this study is illustrated in Fig. 3, and a 3-D schematic view of the system is shown in Fig. 4. Two ellipsoidal reflectors were designed to share common focus where specimen is located and to position the halogen lamps on the other focus in each ellipsoidal reflector for light (or heat) sources. Therefore, when in the test position, the specimen was heated by non-contact radiant light. The distance between the specimen and the halogen lamps was 140 mm. A high temperature ($\sim$1200°C) could be attained in a relatively short amount of time using these reflectors. For example, only 40 s were required to heat an 8-mm long, 8-mm diameter titanium specimen to 1000°C using 90% of the full power of the halogen lamps.

2.2.2. *Temperature measurement*

An infrared thermometer (Raytek Raynger3i; response time: 700 ms, focus point size: 8 mm at 610 mm, measurement range: $-30\sim1200$°C) is used for measuring the temperature of the specimen, which measures the temperature without contacting the specimen. This apparatus may reduce the undesirable disturbance due to the contact. The length and diameter of the specimen

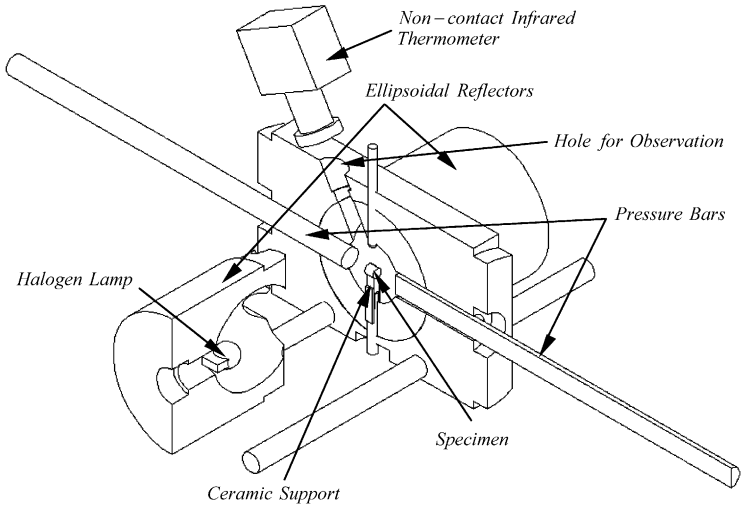

Fig. 4. 3D schematic view of the radiant heating system.

Table 1
Emissivity factors for the Raynger3i thermometer from the Ti–6A1–4V specimen between 200°C and 1000°C

Temperature (°C)	Emissivity (ε)
200	0.67
400	0.47
600	0.43
800	0.50
1000	0.63

were selected to be greater than 8 mm because the smallest focus size of the infrared beam was 8 mm.

The measurement of temperature by using the non-contact thermometer requires the emissivity of an object at a given temperature. The emissivity of a specimen is dependent on the material's surface texture and geometric shape, and on surface conditions such as oxidation, which occurs as the temperature rises. The non-contact thermometer must first be calibrated by obtaining the relationship between the emissivity and temperature of the specimen before measurements can be made. In this study, the readings of thermocouples inserted at the center and near the surface of a specimen as it was heated were compared with the readings of the infrared thermometer. Table 1 lists the emissivity of the Ti–6Al–4V specimens as a function of temperature.

2.2.3. Specimens

A uniform temperature distribution over the entire specimen is required during the high temperature experiment. When the specimen is heated up to the temperature designated for the experiment, the temperature at the surface may increase faster than the internal temperature of

the specimen. The thermal gradient in the specimen will reduce the reliability of the experimental results. Therefore, the specimen temperature was measured at two positions, the center and near the surface, as shown in Fig. 5, to analyze the extent of the thermal gradient. Fig. 6 shows the temperature history at the measurement positions. The pressure bars were located 100 mm from the specimen during heating the specimen. Initially, the radiant heater began to heat the specimen using 90% of the full power of the lamps to reach the experimental temperature as quickly as possible. To prevent a sudden rise in temperature that exceeded the desired experimental value, the power of the heater was reduced to 70% of its full power after 25 s. It took about 40 s to heat the surface of the specimen to 1000°C; at this point, the temperature difference between the two positions was 20°C. After 60 s, the surface temperature of the specimen was about 1050°C, and the difference between the temperature near the surface and in the center of the specimen was less than 5°C.

Before the striker bar impacts the incident bar, the specimen makes contact with the pressure bars. Even though the contact time is less than one second, the surface temperature of the

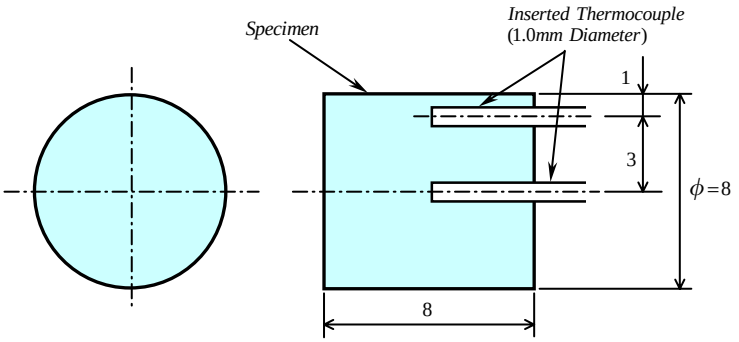

Fig. 5. Test setup to investigate the temperature difference in the specimen.

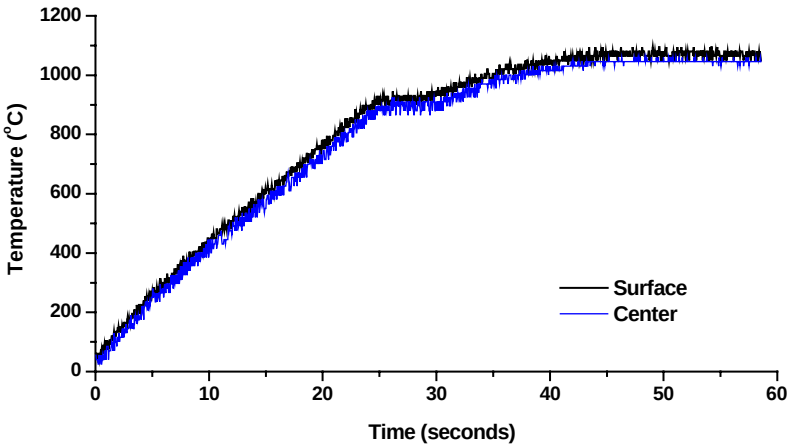

Fig. 6. Temperature increase at the center and near the surface of a specimen.

specimen will drop slightly because of heat conduction to the elastic bars while the inner temperature of the specimen will remain relatively unchanged. Because of this effect, the material strength near the contact surface may be greater than the strength of the internal part of the specimen; the inhomogeneous strength in the specimen may cause an inhomogeneous deformation, such as barreling. This must be investigated to determine how the thermal gradient will effect the material behavior.

Thermocouples were inserted into a specimen, as shown in Fig. 7, to measure the temperature drop during contact with the pressure bars. The pressure bars were initially 100 mm from the specimen. The specimen was then heated for 50 s to a surface temperature of 1025°C. The temperature drop in the specimen was measured when the pressure bars made contact, as shown in Fig. 8. In this figure, the specimen was in contact with the pressure bars at 0.7 s point. After 0.5 s of contact time, the temperature at the center of the specimen was about 1010°C and the temperature near the contact surface was about 990°C. After 1.0 s of contact time, these temperatures dropped to 1000°C and 970°C, respectively. The temperature difference during the actual tests is probably less than 30°C, because the contact time is actually less than 1.0 s. Also, if

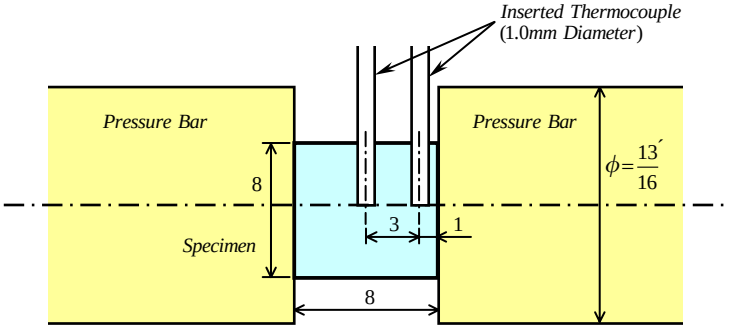

Fig. 7. Setup to measure of the temperature drop in a specimen in contact with the pressure bars.

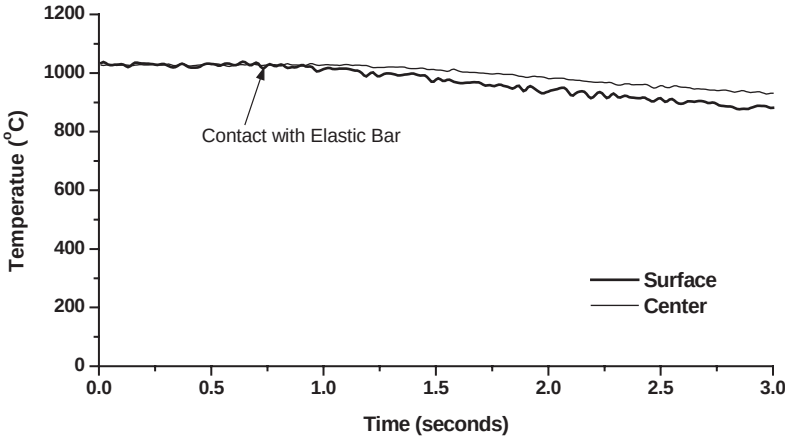

Fig. 8. Temperature drop of a specimen in contact with the elastic bars.

the temperature of the specimen is less than 1000°C after heating at the end surface, the temperature reduction in the specimen during contact between the specimen and pressure bars will decrease, owing to the reduction in the heat conduction. Thus, these preliminary tests demonstrated that the temperature difference between the surface and inner portion of the specimens was less than 30°C.

In this radiant heating system, it is very important that the specimen is positioned properly at the common foci of the two ellipsoidal reflectors, parallel to the cross-section of the pressure bars. Also, it is necessary that the support mechanism of the specimen does not affect the temperature rise in the specimen and does not resist the movement of pressure bars (see Fig. 4). A ceramic board was used to support the specimen. Ceramic board is soft enough for handcrafting and can withstand a large amount of heat. The board can be properly located at the impact position during the heating phase, but it can be broken even by a weak force, such as that generated by the movement of the pressure bars. The length of the ceramic support needs to be shorter than the length of the specimen and the width of the support must be shorter than the diameter of the specimen, because light is concentrated on the specimen from all directions during the heating phase. Thus the specimen surface area covered by the support must be as small as possible.

2.2.4. *Pressure bars*

In the high-temperature SHPB tests, the temperatures at the ends of the pressure bars will be elevated because of heat conduction from the high temperature specimen. The thermal gradient in these end parts will change the Young's modulus, resulting in a change in the mechanical impedance, which may reflect or disperse the waves. If the pressure bar is heated uniformly, wave reflection and dispersion may be avoided; unfortunately, this is almost impossible.

The pressure bars do not make contact with the specimen until the specimen is heated to the designated temperature. Before the striker bar is accelerated toward the incident bar, the pressure bars contact the specimen. Even though the radiant heating system concentrates heat energy on only the specimen, and the pressure bars contact with the specimen for one second at most, some heat conduction to the pressure bars is inevitable.

An inserted thermocouple was used to investigate the temperature rise at the end face of the pressure bars during the contact with the specimen, as shown in Fig. 9. The pressure bars for this test were made of carbon steel (ANSI 1045) rather than Inconel 718. The temperature measurement position was located 1 mm from the end face of the pressure bar. The pressure bars were 100 mm from the specimen during the heating phase. Fig. 10 shows the temperature profile at the end face of the pressure bar during the contact with the high-temperature specimen. When the specimen was heated to 1000°C, the temperature of the end face of the pressure bar was elevated from room temperature to 35°C before contacting the specimen. After contact, the temperature rose to about 60°C in 1.5 s, and to about 90°C in 5 s.

The specific heat capacity of Inconel 718 is similar to that of carbon steel. However, the thermal conductivity of Inconel 718 is less than that of carbon steel. Therefore, the temperature of pressure bars made of Inconel 718 should not exceed that of pressure bars made of carbon steel.

The change in Young's modulus of Inconel 718 with temperature is shown in Fig. 11 [15]. Young's modulus of Inconel 718 drops by 2% when the temperature varies from 21°C to 93°C, which is a sufficient range to cover the change in temperature due to the contact with the high-temperature specimen in this experiment. The specimen and the pressure bars contact just before

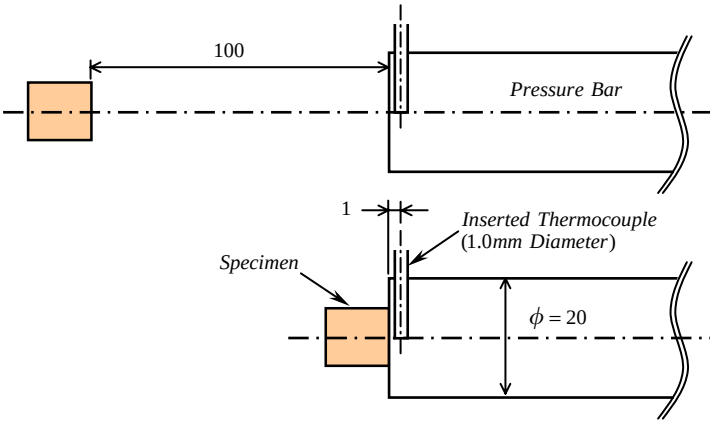

Fig. 9. Test setup to measure the temperature rise at the end faces of pressure bar in contact with specimen.

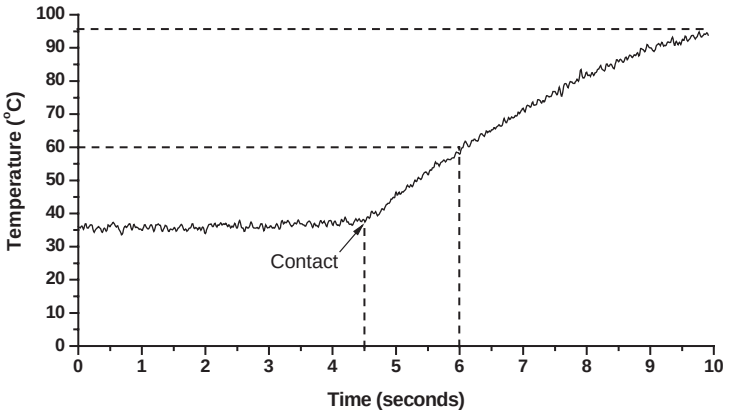

Fig. 10. Temperature profile at the end faces of an ANSI 1045 pressure bar in contact with a specimen at 1000°C.

the impact for as short a length of time as possible. The contact time in the actual experiments was less than 1 s. This analysis indicates that the change in Young's modulus of the pressure bars owing to the rise in temperature may be negligible in this experiment.

2.2.5. Lubrication

Lubrication between the two ends of the specimen and the two pressure bars is related to the barreling effect of the specimen. The barreling phenomenon violates the assumption that deformation occurs uniformly in the SHPB test.

In a test at room temperature at low strain-rates, powdered carbon graphite, compound grease, or solid Teflon are generally used as lubricants, and these have produced very good effects. When barreling occurs in a specimen during a compressive test, the flow stress is greater than that during uniform compression. In a test at high temperatures, the lubrication effects and the strength of the specimen will decrease as the temperature increases. As a result, the effect of barreling may be

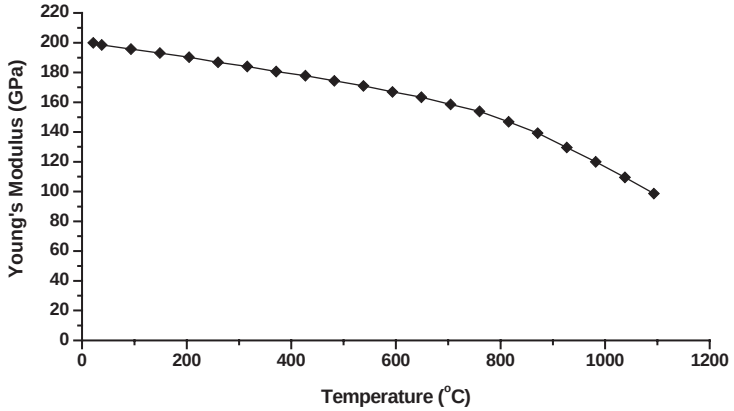

Fig. 11. Change of Young's modulus of Inconel 718 with temperature.

Table 2
Observations of the specimen surface at various temperatures

Temperature (°C)	Color of surface	Oxidation or not	Degree of oxidation
200	Original color	×	×
400	Pale yellow	×	×
600	Stained blue	×	×
800	Deep yellow	O	Partially distributed
1000	Brown	O	Thin film

significant at high temperatures. On the other hand, excessive lubrication can cause distortion and a time delay in the transmitted wave front, because the layer formed at the two ends of the specimen absorbs the propagated stress waves [11–13].

Therefore, the prevention of barreling using lubrication in a high-temperature SHPB test is a very difficult problem to overcome due to the several variables. In this work, a grease containing molybdenum (Mo) was used to reduce the barreling effect.

2.2.6. *Oxidation*

For all types of metal, surface oxidation is caused by reacting oxygen at high temperatures. Since the oxidizing film may disturb the transfer of waves between the pressure bar and specimen in the high-temperature SHPB test, it is necessary to determine the degree and influence of the oxidation when oxidation occurs on a specimen.

Specimens were heated to a specified temperature and maintained at that temperature for two minutes to observe their surface conditions. Changes in the surface color were used to determine the degree of oxidation; these are listed in Table 2. From the results of these tests, there was no oxidation film on the surface of pure titanium specimens at the high temperatures over 1000°C. However, there was a very heavy oxidation film on the surface of high temperature specimens made of materials such as carbon steel. When the surface of a specimen was stained with a

different substance, e.g., lubricating cutting oil, very serious oxidation was generated. On the surface of the Ti–6Al–4V specimen, an oxidation film appeared if the temperature was greater than 1000°C. This oxidation film was thin and uniform over the entire surface. Therefore, wave propagation between the elastic bars and the specimen was not seriously influenced by oxidation in this study.

3. Experiments and results

3.1. Material

The titanium alloy Ti–6Al–4V, AMS 4928N HEAT 579L using the AMS standard, was selected for the specimens in this investigation. This has been used for materials that require high strength, for example, airplane frames, turbine blades, etc. The tests were conducted using a specimen 8 mm in diameter and 8 mm in length. An original specimen and the deformed specimens after the high-temperature SHPB tests are shown in Fig. 12. The specimen tested at 1000°C was excessively compressed and more barreling occurred as compared to any of the other specimens.

3.2. Measurement of the elastic waves

Fig. 13 shows the strain circuit outputs caused by the incident and reflected waves. The strain circuit outputs caused by the transmitted waves are illustrated in Fig. 14. In Fig. 13, the incident waves were reduced as the temperature increased, while the reflected waves, which are related to the strain-rate of the specimen, remained at the same magnitude. This was intentionally caused by a reduction in the velocity of the striker bar in order to maintain the same strain-rate in the different tests. The transmitted waves shown in Fig. 14, which are related to the flow stress of the specimen, changed as the temperature increased. Therefore, the flow stress was reduced as the temperature increased.

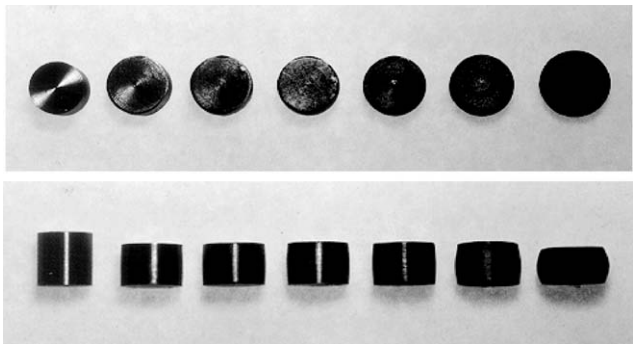

Fig. 12. Deformed shapes after the high-temperature SHPB test: end and side views, original specimen and specimens tested at room temperature, 200°C, 400°C, 600°C, 800°C, and 1000°C.

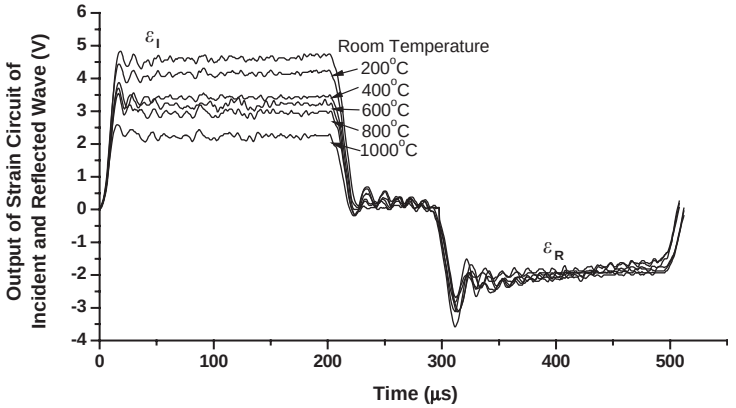

Fig. 13. Strain circuit outputs giving the incident and reflected waves from room temperature to 1000°C.

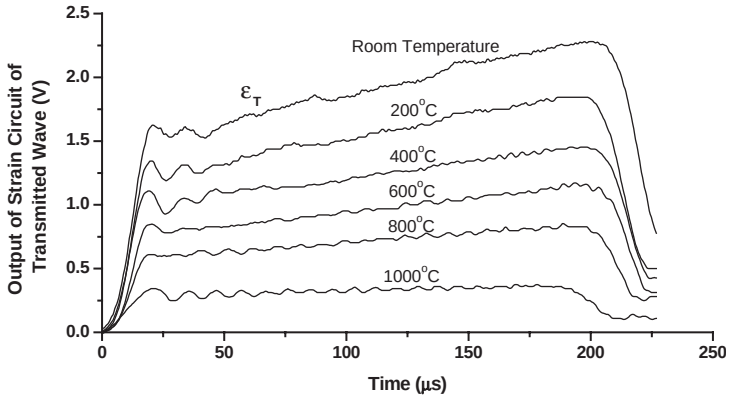

Fig. 14. Strain circuit outputs giving the transmitted waves from room temperature to 1000°C.

3.3. True flow stress–true strain relationship

The true flow stress–true strain relationships of the Ti–6Al–4V titanium alloy between 25°C and 1000°C, at a strain-rate of 1400 s^{-1}, are shown in Fig. 15. The flow stress decreased as the temperature increased. The true stress–temperature relationship at strains of 0.1, 0.15, 0.2, and 0.25 are shown in Fig. 16. The difference between the flow stresses at a given strain decreased as the temperature increased. This indicates that the work hardening effect decreased as the temperature increased. To determine the effect of the strain-rate, a test at a strain-rate of 700 s^{-1} and room temperature was also performed. The results are shown in Fig. 17. The maximum value of the strain and the level of the flow stress at a strain-rate of 700 s^{-1} were lower than those measured at a strain-rate of 1400 s^{-1}.

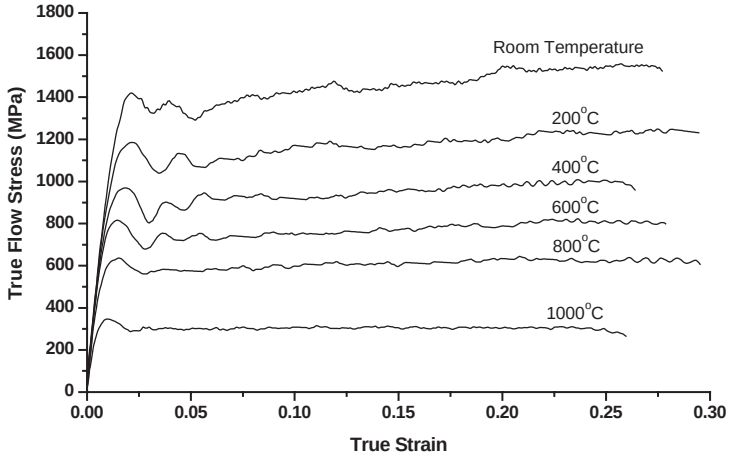

Fig. 15. True flow stress–true strain relationship of Ti–6A1–4V from room temperature to 1000°C at strain-rate 1400 s^{-1}.

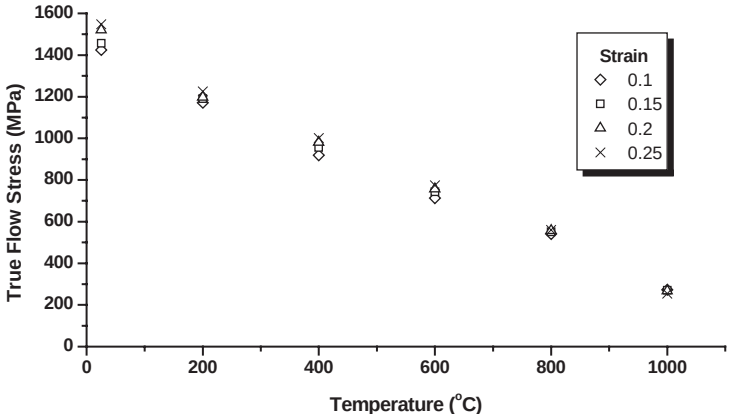

Fig. 16. True flow stress–temperature relationship at strains of 0.1, 0.15, 0.2 and 0.25.

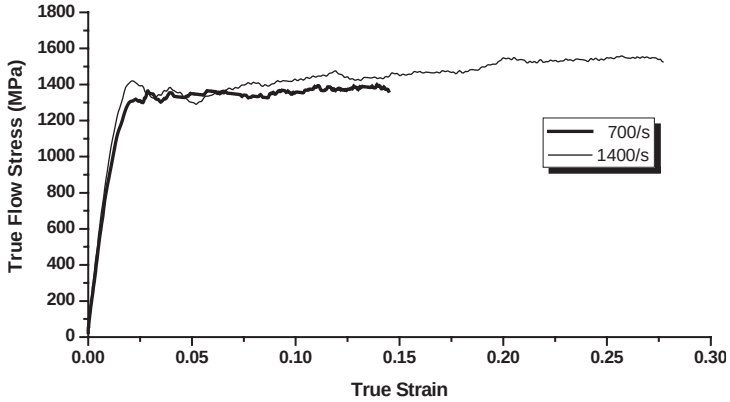

Fig. 17. Flow stresses and strains at two strain-rates and room temperature.

3.4. Johnson–Cook constitutive equation

The temperature-dependent flow stress and strain relationships at a strain-rate of 1400 s^{-1} were equated into the Johnson–Cook constitutive relations to determine the plastic behavior of the Ti–6Al–4V titanium alloy. The five parameters in the Johnson–Cook constitutive equation, A, B, n, C, and m, were used to describe the plastic behavior. This equation consisted of five parameters for the strain, strain-rate, and temperature as follows:

$$\sigma = (A + B\varepsilon^n)\left(1 + C\ln\frac{\dot{\varepsilon}}{\dot{\varepsilon}_0}\right)[1 - (T^*)^m]. \tag{7}$$

The term T^* was defined as

$$T^* = \frac{T - T_r}{T_m - T_r}. \tag{8}$$

The five parameters, A, B, n, C, and m, were calculated from the experimental data and are listed in Table 3. The reference strain $\dot{\varepsilon}_0$ was 1 s^{-1} and the reference temperature T_r was room temperature, 25°C. The melting temperature T_m for Ti–6Al–4V is 1668°C [16]. Thus, Eq. (8) can be rewritten as

$$T^* = \frac{T - 25}{1668 - 25} = \frac{T - 25}{1643}. \tag{9}$$

A comparison of the Johnson–Cook constitutive equation and the experimental data for the Ti–6Al–4V alloy is shown in Fig. 18. The figure indicates that the Johnson–Cook constitutive equation is in reasonable agreement with the experimental data from room temperature to 600°C, but there is a significant difference between the two sets of data at 800°C and 1000°C.

3.5. Modified Johnson–Cook constitutive equation

A modified Johnson–Cook constitutive equation was proposed by Andrade and Meyers [17]. They added a term to account for the change in the stress due to a phase transformation above the recrystallization temperature. The modified constitutive equation is

$$\sigma = (A + B\varepsilon^n)\left(1 + C\ln\frac{\dot{\varepsilon}}{\dot{\varepsilon}_0}\right)[1 - (T^*)^m]H(T), \tag{10}$$

where $H(T)$ is defined as

$$H(T) = \frac{1}{1 - [1 - \frac{(\sigma_f)_{rec}}{(\sigma_f)_{def}}]u(T)}, \tag{11}$$

Table 3
The five parameters of the Johnson–Cook constitutive equation for Ti–6A1–4V

A (MPa)	B (MPa)	n	C	m
997.9	653.1	0.45	0.0198	0.7

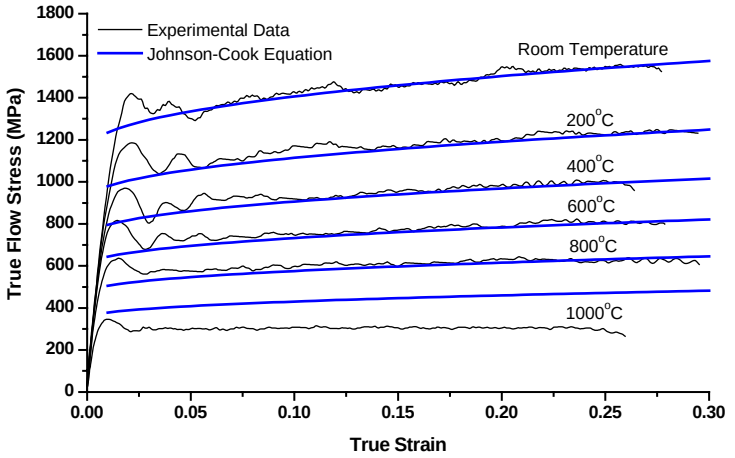

Fig. 18. Comparison of the true flow stress–true strain relationship of Ti–6Al–4V for the experimental data and the Johnson–Cook constitutive equation.

$(\sigma_f)_{rec}$ and $(\sigma_f)_{def}$ are the flow stresses just prior to and after recrystallization, respectively, and $u(T)$ is a step function of the temperature, defined as

$$u(T) = \begin{cases} 0 & \text{when } T < T_C, \\ 1 & \text{when } T > T_C, \end{cases} \tag{12}$$

where T_C is the recrystallization temperature. Eqs. (10)–(12) can be simplified into

$$\sigma = (A + B\varepsilon^n)\left(1 + C\ln\frac{\dot{\varepsilon}}{\dot{\varepsilon}_0}\right)[1 - (T^*)^m] \quad \text{when } T < T_C, \tag{13}$$

$$\sigma = (A + B\varepsilon^n)\left(1 + C\ln\frac{\dot{\varepsilon}}{\dot{\varepsilon}_0}\right)[1 - (T^*)^m]\frac{(\sigma_f)_{def}}{(\sigma_f)_{rec}} \quad \text{when } T > T_C, \tag{14}$$

Eq. (13) is the same as the Johnson–Cook constitutive equation, but Eq. (14) has been modified by adding a ratio of the flow stresses just prior to and following recrystallization. The recrystallization temperature of titanium alloy is 995 ($\pm$15)°C; the alloy transforms from α–β phase to β phase at that temperature. Additional tests at temperatures of 900°C, 950°C, and 1100°C were performed to verify that there was a decrease in the flow stress at temperatures greater than the recrystallization temperature. A drastic drop in the flow stress occurred between 950°C and 1000°C, corresponding to the expected range of the recrystallization temperature. If the recrystallization temperature of the titanium alloy was about 995°C, the flow stresses just prior to and after recrystallization can be obtained from the data shown in Fig. 19. This gives $(\sigma_f)_{rec}$ and $(\sigma_f)_{def}$ as 442.3 MPa and 288.2 MPa, respectively, and a corresponding $H(T)$ of 0.65. The parameters for the modified Johnson–Cook equation when $T < T_C$ and $T > T_C$ are listed in Table 4. The two Johnson–Cook equations are shown in Fig. 20 with the experimental data. The modified Johnson–Cook constitutive equation describes the experimental results better than the Johnson–Cook equation when $T > T_C$.

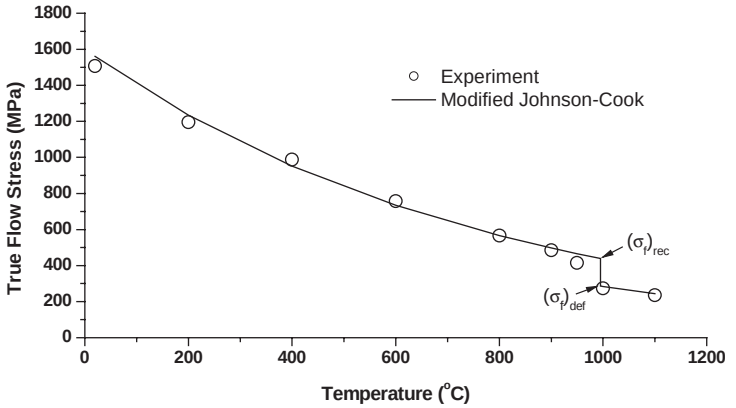

Fig. 19. Change of the true flow stress due to temperature at a strain of 0.2.

Table 4
The five parameters of the modified Johnson–Cook constitutive equation for Ti–6Al–4V

Condition	A (MPa)	B (MPa)	n	C	m	$H(T)$
$T < T_C$	997.9	653.1	0.45	0.0198	0.7	1.0
$T > T_C$	997.9	653.1	0.45	0.0198	0.7	0.65

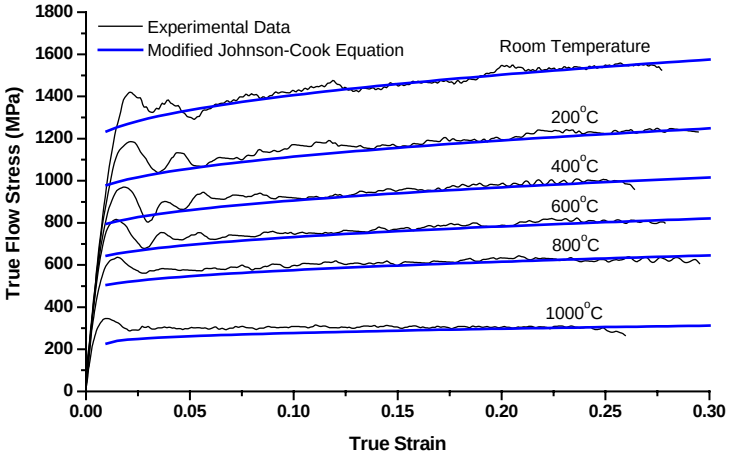

Fig. 20. Comparison of the true flow stress–true strain relationship of Ti–6Al–4V for the experimental data and the modified Johnson–Cook constitutive equation.

3.6. Effects of friction and adiabatic heating

In Fig. 12, which shows the shapes of deformed specimens after the test, it can be seen that the barreling effect grew as the temperature increased. This was because the lubricant

that was used to reduce friction oxidized at high temperatures. Malinowski et al. [18] tried to correct the stress due to friction through an energy balance approach. They proposed the following relation:

$$\sigma_c = \left[1 - \frac{\mu}{S_0}(1-\varepsilon)^{-3/2}\right]\sigma_e, \tag{15}$$

where σ_c denotes the true material response during plastic flow, σ_e is the compressive stress determined from the experiment, μ is the coefficient of Coulomb friction, $S_0 = D_0/L_0$ is the slenderness ratio, and ε is the strain. This relation was applied to the flow stresses obtained at 800°C and 1000°C, tests in which the frictional effect appeared to be significant. Since the friction between the bars and the specimen was caused by metal-on-metal, reasonable values were selected from those estimated by Hawkyard and Freeman, 0.02–0.06 (cited in [6]), under conditions that were similar to the present experiment. The exact coefficients of friction at each elevated temperature were difficult to estimate, so they were assumed to be $\mu = 0.03$ for 800°C and $\mu = 0.06$ for 1000°C, because the effect of friction was expected to increase with temperature. The results are shown in Fig. 21. In the figure, broken lines give the results with no stress correction, which are slightly different from the corrected curve. However, the results with frictional correction are not very different from the results given by the modified Johnson–Cook equation.

Adiabatic heating should also be considered. When plastic deformation occurs in a material under a very high strain-rate and strain, a large proportion of the work done may be converted into heat. This adiabatic heating effect will increase the temperature in the specimen, thereby reducing the flow stress [19]. However, if the strain-rate is relatively low ($1400 \sim 1500\ s^{-1}$) and the strain is less than 0.3, the effect of the increased temperature due to adiabatic heating will be insignificant or small.

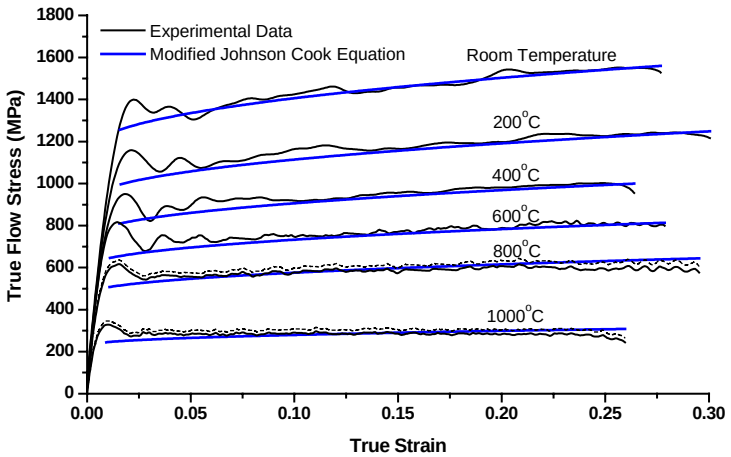

Fig. 21. Comparison of the true flow stress–true strain relationship of Ti–6Al–4V for the experimental data and the modified Johnson–Cook constitutive equation when a stress correction for friction is included at 800°C and 1000°C (broken line: no correction for friction).

4. Conclusions

We introduced a new experimental technique for a high-temperature SHPB test system. Temperatures of up to 1100°C were attained using two ellipsoidal aluminum reflectors with two halogen lamps. Unlike other types of furnace, this radiant heating system prevents annealing and aging effects in the pressure bars. The specimens could be elevated to very high temperatures ($\sim$1100°C) in a short time. An infrared thermometer was used to measure the temperature of the specimens without any contact. This non-contact technique has several merits: the temperature of the specimen can be measured more accurately, and undesirable disturbances caused by contact between the thermometer and specimen can be reduced.

Temperature variations caused by contact between the pressure bars and the specimen were investigated using inserted thermocouples. To increase the reliability of the experimental results, the thermal gradients in the specimen were also investigated, both during the heating phase and when the specimen was in contact with the pressure bars. The specimen and the pressure bars contacted only just before the impact in order to reduce the length of the contact time to less than 1 s. The variation of Young's modulus in the pressure bars due to the contact with the high temperature specimen was negligible in this experiment.

The high-temperature SHPB test was used to determine the true flow stress–true strain relationship of the Ti–6A–4V titanium alloy between room temperature and 1000°C, at intervals of 200°C, at a strain-rate of approximately 1400 s^{-1}. The tests showed that as the temperature increased, the flow stresses and the work hardening effects decreased. However, for high temperatures, such as 800°C and 1000°C, oxidation and evaporation of the lubricant resulted in increasing frictional effects. Therefore, a correction was made to the measured stresses at these temperatures. Although the corrected stresses were somewhat lower than the original stresses, the corrected curve did not deviate greatly from the original curve that was plotted using the modified Johnson–Cook constitutive equation. Even when frictional effects were considered, the modified Johnson–Cook constitutive equation was more suitable for expressing the dynamic behavior of Ti–6Al–4V than the original Johnson–Cook constitutive equation at temperatures greater than the recrystallization temperature.

Acknowledgements

This work was supported by Grant No. RO1-2001-000-00390-0(2002) from the Basic Research Program of the Korea Science & Engineering Foundation.

References

[1] Lindholm US. Some experiments with the split Hopkinson pressure bar. J Mech Phys Solids 1964;12:317–35.
[2] Follansbee PS. The Hopkinson bar. ASM handbook. vol. 8, 9th ed. Materials Park, OH: ASM International; 1985. pp. 198–203.
[3] Follansbee PS, Flantz CE. Wave propagation in the split Hopkinson pressure bar. J Eng Mater Technol 1983;105:61–6.

[4] Hopkinson B. A method of measuring the pressure produced in the detonation of high explosive or by the impact of bullets. Philos Trans Roy Soc London Series A 1914;213:437–56.
[5] Kolsky H. An investigation of the mechanical properties of materials very high rates of loading. Proc Phys Soc (London) 1994;B63:676–700.
[6] Davies EDH, Hunter SC. The dynamic compression testing of solids by the method of the split Hopkinson pressure bar. J Mech Phys Solids 1963;11:155–79.
[7] Chiddister JL, Malvern LE. Compression–impact testing of aluminum at elevated temperature. Exp Mech 1963;3:81–90.
[8] Lankford J. Temperature-strain rate dependence of compressive strength and damage mechanisms in aluminum oxide. J Mat Sci 1981;16:1567–78.
[9] Lee WS, Lin CF. High-temperature deformation behavior of Ti6Al4V alloy evaluated by high strain-rate compression tests. J Mater Process Technol 1998;75:127–36.
[10] Lee WS, Yeh GW. The plastic deformation behavior of AISI 4340 alloy steel subjected to high temperature and high strain rate loading conditions. J Mater Process Technol 1997;71:224–34.
[11] Lennon AM, Ramesh KT. A technique for measuring the dynamic behavior of materials at high temperatures. Int J Plasticity 1998;14(12):1279–92.
[12] Macdougall D, Harding J. The measurement of specimen surface temperature in high-speed tension and torsion tests. Int J Impact Eng 1998;21:473–88.
[13] Macdougall D. A radiant heating method for performing high-temperature high-strain-rate tests. Meas Sci Technol 1998;9:1657–62.
[14] Yang H, Min O, Park K. Temperature dependence of dynamic behavior of titanium by the high strain-rate compression test. Proceeding of the Fourth International Symposium on Impact Engineering, 16–18 July 2001, Kumamoto, Japan, vol. II, 571–6.
[15] Publication Number SMC-045. Special Metals Corporation 2002 (Sep02).
[16] Myer Kutz. editor. Mechanical Engineers' Handbook, 2nd ed. New York: Wiley; 1998.
[17] Andrade UR, Meyers MA, Vecchio KS, Chokshi AH. Dynamic recrystallization in high-strain, high-strain-rate plastic deformation of copper. Acta Metall Mater 1994;42:3183–95.
[18] Malinowski JZ, Klepaczko JR. A unified analytic and numerical approach to specimen behavior in the split-Hopkinson pressure bar. Int J Mech Sci 1986;28(6):381–91.
[19] Mason JJ, Rosakis AJ, Ravichandran G. On the strain and strain rate dependence of the fraction of plastic work converted to heat: an experimental study using high speed infrared detectors and Kolsky bar. Mech Mater 1994;17:135–45.